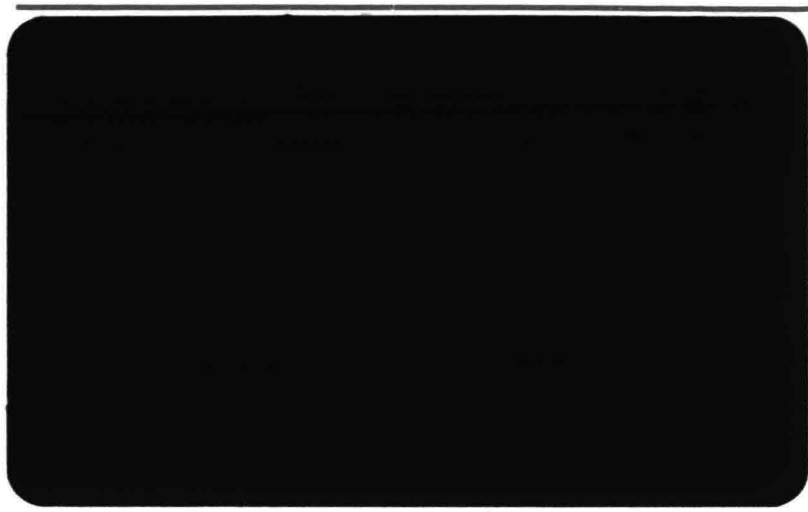

TU Delft
Delft University of Technology

Faculty of Civil Engineering
Department Hydraulic Engineering

Local scour
Flow model with prescribed eddy viscosity

Report nr. 11-88 Volume 1

G.J.C.M Hoffmans

Text

Faculty of Civil Engineering
Hydraulic Engineering
Delft University of Technology

1988

Summary

A two dimensional mathematical model DUCT, which is based on a parabolic boundary layer technique, using finite elements, is proposed to predict the flow and turbulence field in complicated geometrical conditions, where recirculating flow may occur.
Numerical results of the DUCT-model are compared with k-ϵ-predictions as well as laboratory experiments concerning the flow in a number of configurations.
In the case of a steep lee-side the location of the separation point is not well located, because the normal stresses in the equation of motion are neglected. Generally the velocities in the deceleration and acceleration zone are satisfactory.
An advantage of the application of the DUCT-model compared with the sophisticated k-ϵ-model is the relatively low computation time used to solve the set of equations.

Contents

Notation

a	= flow depth	(L)
B	= width of flume	(L)
c_b	= bottom coefficient (deceleration zone)	(-)
c_p	= dimensionless pressure coefficient (on rigid lid)	(-)
c_λ	= empirical constant (relaxation zone)	(-)
C	= Chezy coefficient	$(L^{1/2}T^{-1})$
D_{50}	= mean particle size	(L)
f	= roughness parameter or function	(-)
Fr	= Froude number	(-)
g	= acceleration of gravity	(LT^{-2})
i	= slope of the coordinate system or energy slope	(-)
k_s	= equivalent roughness of Nikuradse	(L)
l_m	= mixing length of Prandtl	(L)
L	= length scale of turbulence	(L)
L_x	= roughness parameter	(-)
n	= integer, index	(-)
m	= integer, index	(-)
$\bar{p}$	= time-averaged pressure	$(ML^{-1}T^{-2})$
q	= discharge per unit width	(L^2T^{-1})
R	= hydraulic radius	(L)
R_b	= hydraulic radius; corrected for side-wall influences	(L)
Re	= Reynolds number	(-)
$\bar{u}$	= local time-averaged longitudinal flow velocity	(LT^{-1})
u'	= longitudinal flow velocity fluctuation	(LT^{-1})
u_*	= bed-shear velocity	(LT^{-1})
$u_{*,b}$	= overall bed-shear velocity	(LT^{-1})
$\bar{U}$	= depth-averaged longitudinal flow velocity	(LT^{-1})
v	= transverse flow velocity	(LT^{-1})
$\bar{w}$	= local time-averaged vertical flow velocity	(LT^{-1})
w'	= vertical flow velocity fluctuation	(LT^{-1})
x	= longitudinal coordinate	(L)
y	= transverse coordinate	(L)
z	= vertical coordinate	(L)
z_0	= zero-velocity level	(L)

Notation (continued)

α_b	= rotation angle (bottom slope)	(-)
α_m	= mixing layer parameter	(-)
α_w	= exponential parameter	(-)
α_ν	= damping exponent eddy viscosity (relaxation zone)	(-)
β	= angle mixing layer	(-)
ψ	= growth-factor mixing layer	(-)
$\bar{\lambda}$	= averaged damping constant (relaxation zone)	(L)
κ	= Von Karman's universal constant	(-)
ν	= kinematic molecular coefficient	$(L^2 T^{-1})$
ν_t	= eddy viscosity	$(L^2 T^{-1})$
ρ	= fluid density	(ML^{-3})
θ	= momentum thickness of a boundary layer	(L)
σ_ν	= standard deviation (eddy viscosity)	(-)
τ_t	= turbulent shear stress	$(ML^{-1}T^{-2})$
τ_o	= bed-shear stress	$(ML^{-1}T^{-2})$
δ	= laminar sub-layer thickness	(L)
δ_t	= distance from the wall (turbulent region)	(L)
δ_m	= thickness mixing layer	(L)
δ_w	= thickness new wall-boundary layer	(L)
$\bar{\zeta}$	= time-averaged pressure on rigid lid	$(ML^{-1}T^{-2})$
Π	= Coles's profile parameter of boundary layer	(-)

Subscripts

o	= initial section; transition from uniform flow (fixed bed) to deceleration zone (erodible bed)
b	= bed
e	= equilibrium value
max	= maximum
n	= normal-direction (perpendicular to flow direction)
ref	= reference height
R	= reattachment point
w	= at outer edge of new wall-boundary layer

Subscripts (continued)

η = relaxation point; transition from deceleration zone to relaxation zone

τ = tangential (parallel to flow direction)

Abbreviations

D = Dune

LS = Local scour hole

T = Trench

1. Introduction

The general purpose of this research project is to model mathematically the scouring hole downstream of a structure (2-D). The model has to simulate the development of the scour as a function of time.
Basically two models are necessary namely a flow model and a morphological model. The latter has to describe the bed- and the suspended load and the erosion of the bed.
In the present study a mathematical flow model is described which is in principle based on the momentum equation for turbulent flow and the equation of continuity. The eddy viscosity is prescribed according to existing theories of a uniform flow, a mixing layer (deceleration zone), the development of a new wall-boundary layer and a lagging or damping turbulent flow (relaxation zone).
Computations of the k-ϵ-model ODYSSEE concerning the flow in a number of local scour holes (Hoffmans, 1988a) and experimental data, Laser Doppler velocity measurements, concerning the flow of two artificial dunes (van Mierlo and de Ruiter, 1988) and two trenches (van Rijn, 1980) have been used to calibrate the eddy viscosity distribition.
The mathematical and numerical modelling of the k-ϵ-model has been carried out by Delft Hydraulics, in co-operation with the 'Laboratoire National d'Hydraulique', a department of the 'Electricité de France' Chatou in France.
The DUCT-model with the mixing length theorem of Prandtl has been developed by Vreugdenhil (1982), while the extension of this model (prescribed eddy viscosity) has been performed by Hoffmans, Delft University of Technology, Department of Civil Engineering.
The project is sponsored by Rijkswaterstaat, Ministry of Public Works of the Netherlands.
The present report has been composed by G.J.C.M Hoffmans.

2. DUCT-model

2.1 Assumptions and equations

A steady two-dimensional flow is considered. The usual boundary-layer assumptions are made, i.e.

- the vertical accelerations are small so that a hydrostatic pressure distribution applies.
- horizontal gradients of a parameter are neglected in comparison with vertical gradients.

In addition, the rigid-lid approximation is made, in which the free surface is replaced by a fixed (free-slip) boundary on which a non-zero pressure may result. The latter is a measure of the surface elevation, which would occur if the surface were free. In order to account for the general surface slope, the rigid lid is assumed to be non-horizontal.

The coordinate system and some definitions are given in figure 1. It is assumed that the flow-configuration is infinetely long and that the transverse flow velocity ($\bar{v}$; in y-direction) is equal to zero.

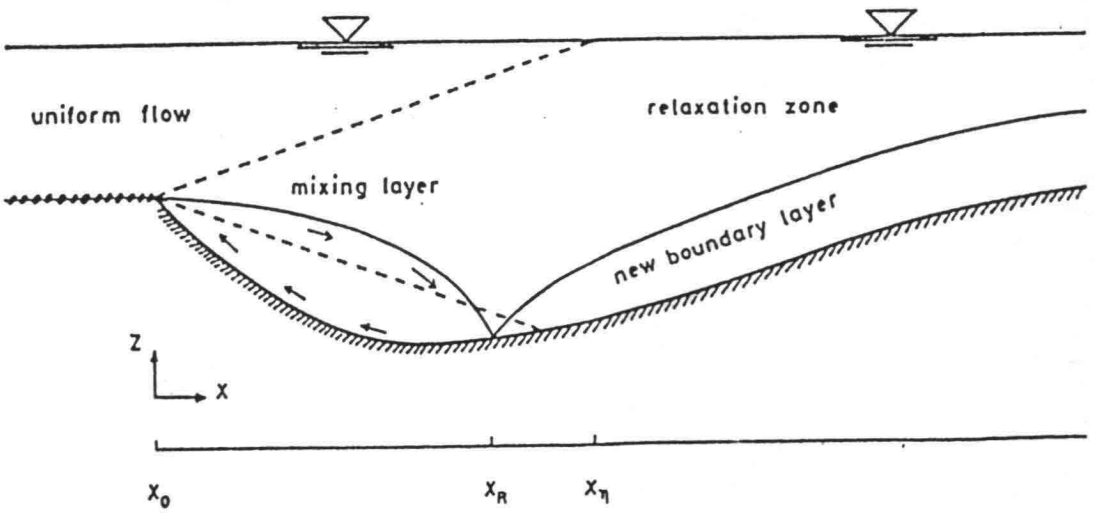

figure 1 Coordinate system and definitions

Neglecting the viscous stresses, the equations of continuity and motion can be solved numerically provided the eddy viscosity is specified. With the above assumptions, the following set of equations is found:

continuity

$$\frac{\partial \bar{u}}{\partial x} + \frac{\partial \bar{w}}{\partial z} = 0 \qquad (1)$$

x-momentum

$$\bar{u}\frac{\partial \bar{u}}{\partial x} + \bar{w}\frac{\partial \bar{u}}{\partial z} = -\frac{\partial \bar{\zeta}}{\rho \partial x} + \frac{\partial}{\partial z}\{\nu_t \frac{\partial \bar{u}}{\partial z}\} + gi \qquad (2)$$

z-momentum

$$\bar{p} = \bar{\zeta} + \rho g(a - z) \qquad (3)$$

in which:

a = flow depth
g = acceleration of gravity
i = slope of the coordinate system and rigid lid
$\bar{p}$ = time-averaged pressure
$\bar{u}$ = local time-averaged longitudinal flow velocity
$\bar{w}$ = local time-averaged vertical flow velocity
x = longitudinal coordinate
z = vertical coordinate
ν_t = eddy viscosity
ρ = density fluid
$\bar{\zeta}$ = time-averaged pressure on rigid lid

2.2 Boundary conditions

2.2.1 Inflow boundary

At the inflow boundary uniform flow conditions are applied. Assuming a logarithmic flow velocity profile and a hydrostatic pressure distribution, this results in a parabolic distribution of the eddy viscosity. If the bottom at the inflow boundary is rough, the following equations apply:

$$\bar{u}(z) = \frac{u_*}{\kappa} \ln \frac{z}{z_0} \tag{4}$$

$$\nu_t(z) = \kappa u_* z(1 - \frac{z}{a_0}) \tag{5}$$

$$u_* = \frac{\bar{U}_0\sqrt{\bar{g}}}{C} \tag{6}$$

$$C = 18\log\frac{12a_0}{k_s} \quad ; \quad \text{(hydraulic rough)} \tag{7}$$

in which:

a_0 = flow depth at $x = x_0$

C = Chezy coefficient

k_s = equivalent roughness of Nikuradse

u_* = bed-shear velocity

$\bar{U}_0$ = depth-averaged flow velocity at $x = x_0$

x_0 = initial section; transition from uniform flow (fixed bed) to deceleration zone (erodible bed)

$z_0 = 0.033k_s$; zero-velocity level

$\kappa = 0.4$; Von Karman's universal constant

2.2.2 Surface

The computations will be made for small values of the Froude number. At the free surface the boundary conditions are:

$$\bar{w} = 0 \tag{8}$$

$$\frac{\partial\bar{u}}{\partial z} = 0 \quad \text{(free slip)} \tag{9}$$

2.2.3 Bottom

At the bottom, a no slip condition is applied, which together with the condition of impermeability leads to:

$$\bar{u} = \bar{w} = 0 \qquad \text{at } z = z_b(x) + z_0 \tag{10}$$

In which z_b is the bed coordinate.

The determination of the bed-shear stress has been realised by:

$$\tau_0/\rho = \kappa^2 \frac{\bar{u}_\tau(\delta_{t,\tau})|\bar{u}_\tau(\delta_{t,\tau})|}{\ln^2\{\delta_{t,\tau}/z_0\}} = u_*|u_*| \tag{11}$$

in which:

τ_0 = bed-shear stress

$\bar{u}_\tau(\delta_{t,\tau}) = \sqrt{[\bar{u}^2(\delta_{t,z}) + \bar{w}^2(\delta_{t,z})]}$; tangential velocity (12)

$\delta_{t,\tau}$ = distance from the wall beyond which the flow is completely turbulent; (perpendicular to the bottom)

$\delta_{t,z}$ = distance from the wall; (z-direction)

$z_0 = 0.033k_s$ (rough); $u_*k_s/\nu \geq 70$ (13)

$z_0 = 0.11\nu/u_* + 0.033k_s$ (general); $5 < u_*k_s/\nu < 70$ (14)

$z_0 = 0.11\nu/u_*$ (smooth); $u_*k_s/\nu \leq 5$ (15)

$\nu = 10^{-6}$ m^2/s; kinematic molecular coefficient

If the wall is not rough the solution is calculated by iteration. It should be noted that the prediction of the bed-shear velocity at the transitions of a smooth-/general- and a general-/rough region is discontinuous, although the discontinuities are relatively small.

2.2.4 Outflow boundary

Because the computation is progressing in a 'parabolic' way marching in the flow direction no boundary conditions are needed at the outflow section.

A detailed description of the numerical procedure such as the mesh generation, the solution of the equations is given by Vreugdenhil (1982). It is based on a parabolic boundary layer technique (explicit scheme) using finite elements.

3. Modelling of eddy viscosity

In a local scour the following characteristic zones can be distinguished; mixing layer (deceleration-), relaxation zone and a new wall-boundary layer (acceleration zone), figure 1.

Nature of the flow

In the deceleration zone, after the transition from a fixed bed to an erodible bed, the separated shear layer appears to be much like an ordinary plane mixing layer. The center of the mixing layer is slightly curved.
Due to the relatively steep lee-side (1:1 to 1:2) a wake zone will develop with a flow direction opposite to the mean flow direction. Then the separated shear layer curves sharply downwards in the reattachment zone and impinges on the wall. Part of the shear-layer fluid is deflected upstream into the recirculation flow by a strong interaction with the wall in the reattachment zone.
The recirculating flow region below the shear layer (wake zone) cannot be characterised as a dead air zone. The maximum measured backflow velocity is usually over 20% of the free stream velocity. Also very large turbulent structures with length scales pass through the reattachment region.
Downstream of reattachment (relaxation zone) a rapid decay of Reynolds normal and shear stresses occur. Simultaneously, a new wall-boundary layer begins to grow up through the reattached shear layer. At some distance downstream the turbulent shear layer reattaches to the surface.

Modelling of the flow

The center of the mixing layer is located at the height of the old bottom-configuration. The flow above the mixing layer, where uniform flow conditions are dominating, is more or less in equilibrium.
The mixing layer spreads outwards at a relatively small angle as indicated in figure 1. The thickness of the mixing layer is proportional to the longitudinal distance and reaches its maximum if it is equal to

the local flow depth. Then the turbulence decreases into the downstream direction (relaxation zone).
After the reattachment point or if the gradient of the longitudinal flow velocity to z ($\partial\bar{u}/\partial z$) has reached its minimum, a new wall-boundary layer will develop. The flow is more or less in equilibrium again in case the boundary layer thickness is equal to the local flow depth. The thickness of the lagging or damping turbulent flow (above the new-wall boundary layer) is decreasing by the development of the new wall-boundary layer. Mostly the transitions mentioned above will overlap; reattachment point/relaxation point, i.e. the transition from the deceleration- to the relaxation zone. Particularly the form of the configuration and the angle of the mixing layer determine the relaxation point, while the reattachment point is determined by the generated flow velocity field.

3.1 Deceleration zone

The eddy viscosity at the center of the mixing layer increases with, (Kay and Nedderman, 1986):

$$\nu_t(x) = \psi \bar{U}_0 \delta_m(x) \tag{16}$$

in which:
ψ = 0.010 to 0.020; growth-factor mixing layer
$\delta_m = \beta x$; thickness mixing layer
β = 0.175 to 0.225; angle of mixing layer

Based on the results of the turbulence model ODYSSEE (Hoffmans, 1988a) and the Laser Doppler measurements (van Mierlo and de Ruiter, 1988 and van Rijn, 1980) the distribution of the eddy viscosity in the vertical direction is modelled by a Gaussion-function.

$$\nu_t(x,z) = \nu_t(x)\, f_b(z)\, \underbrace{\exp\left\{-\alpha_m \frac{\{z - (a(x) - a_0)\}^2}{\delta_m^2(x)}\right\}}_{\text{Gaussion function}} \tag{17}$$

in which:

$f_b = \tanh\{c_b \frac{z}{a}\}$; correction function (bottom: $\nu_t = 0$) (18)

$\alpha_m = 0.25$; mixing layer parameter

$c_b = 10$ to 100; bottomcoefficient

Close to the bottom the function $f_b(z)$ is used to press the value of the eddy viscosity to zero, so it has a small influence region on the distribution of the eddy viscosity. The mixing layer parameter α_m determines the form of the eddy viscosity profile. By a diminution of α_m (or an increase of the mixing layer thickness) the diffusion increases in the entire vertical, while by an enlargement the diffusion is restricted to the center of the mixing layer. Then close to the bottom the value of the eddy viscosity is very small.
If δ_m reaches its maximum, the form of the Gaussion function is so much leveled, that the eddy viscosity has a nearly constant value in the relaxation zone (flow above the new wall-boundary layer).
Above the mixing layer ($z > z_b + a - a_0 + \delta_m$) the eddy viscosity is written by a parabolic function according to the equations (5), (6) and (7). Although there is a discontinuity in the modelling of the viscosity between the mixing layer and the layer above (uniform flow), the discontinuity is relatively small.

3.2 Relaxation zone

After the mixing layer thickness (δ_m) has reached its maximum, the eddy viscosity decreases in the longitudinal direction, (Hoffmans, 1988b):

$$\nu_t(x) = \underbrace{\nu_{t,\eta}}_{1} \underbrace{\{\frac{x - x_\eta}{\bar{\lambda}} + 1\}^{\alpha_\nu}}_{2} \quad ; \quad x > x_\eta \tag{19}$$

in which:

$\nu_{t,\eta} = \psi \bar{U}_0 a_\eta$; eddy viscosity at $x = x_\eta$ (20)

a_η = flow depth at x_η

x_η = relaxation point: transition from the deceleration- to the relaxation zone

$\bar{\lambda} = c_\lambda \frac{a_0}{a_\eta} x_\eta$; averaged damping constant (21)

c_λ = 2.5; empirical coefficient

α_ν = -0.087; damping-exponent eddy viscosity (relaxation zone)

Term 1 in equation (19) represents the maximum value of the eddy viscosity at the relaxation point, while term 2 characterizes the damping of the eddy viscosity in the relaxation zone.

3.3 New wall-boundary layer

Downstream of reattachement a new wall-boundary layer will develop. The turbulent thickness of the boundary layer is given by, (appendix A):

$$\frac{d\delta_w(x)}{dx} = \frac{\kappa^2}{L_x - 2} \quad ; x > x_R \tag{22}$$

in which:

δ_w = thickness new wall-boundary layer

x_R = reattachment point; transition from the deceleration zone to the new wall-boundary layer

$L_x = \ln(\delta_w/z_0)$ = 5 to 11; roughness parameter

The roughness parameter L_x ranges from 5 to 11, so the flow is in equilibrium (uniform flow conditions) at a distance of 20 to 50 times the flow depth (after reattachment point). The boundary layer thickness increases degressively to the flow direction. In case of a rougher bottom the boundary layer will grow faster.
Based on measurements above artificial dunes (van Mierlo and de Ruiter, 1988), figure 2, the eddy viscosity in a new wall-boundary layer with a turbulent outer flow is modelled by, (Hoffmans, 1988c):

$$\nu_t(z) = \kappa u_* z \exp(-\frac{\alpha_w z}{\delta_w}) \qquad 0 < \frac{z}{\delta_w} < \frac{z_{ref}}{\delta_w} \tag{23}$$

$$\nu_t(z) = \nu_{t,w} - (\nu_{t,w} - \nu_{t,ref})\exp\{-[\frac{\frac{z}{\delta_w} - \frac{z_{ref}}{\delta_w}}{\sigma_\nu}]^2\} \; ; \; \frac{z_{ref}}{\delta_w} < \frac{z}{\delta_w} < 1 \quad (24)$$

in which:

α_w = exponential parameter
$\nu_{t,w}$ = eddy viscosity at outer edge of boundary layer
$\nu_{t,ref}$ = eddy viscosity at reference heigth
z_{ref} = reference heigth
σ_ν = standard deviation (eddy viscosity)

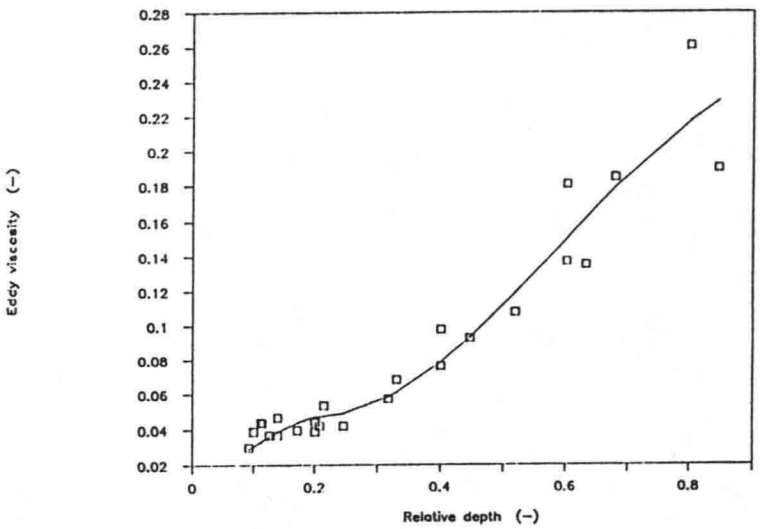

□ Measurements (Delft Hydraulics, 1988)
——— according to (23) and (24)
$\alpha_w = 2.6$, $z_{ref}/\delta_w = 0.2$, $\sigma_\nu = 0.52$

figure 2 Eddy viscosity: boundary layer with disturbed outer flow

Equation (23) describes the eddy viscosity reasonably well near the wall, where L (= length scale of turbulence) is relatively small (ν_t :: L). Then the eddy viscosity reads:

$$\nu_t = \kappa u_* z \quad ; \quad z << \delta_w \quad (25)$$

Assuming a logarithmic flow velocity profile this is in agreement with the theorem of Prandtl.

Prandtl: $\tau_{t,xz} = \rho l_m^2 \{\frac{\partial \bar{u}}{\partial z}\}^2$ (26)

in which:

$\tau_{t,xz}$ = turbulent shear stress

$l_m = \kappa z$; mixing length of Prandtl

Above z_{ref} (reference heigth) the turbulence level in the new wall-boundary layer is influenced by the turbulence level in the outer flow (layer above the new wall-boundary layer). The relative high turbulence level is caused by a developed mixing layer upstream.
The present calculations (DUCT-model) are carried out with:

General: $\alpha_w = 2.5$; $\sigma_\nu = 0.45$; $z_{ref}/\delta_w = 0.25$

Dunes/Trenches: $L_x = 5.0$ (rough, $k_s = 2.5/6*10^{-3}$ m)

Local scour holes: $L_x = 8.0$ (smooth, $k_s = 0.5*10^{-3}$ m)

4. Applications

4.1 Local scour holes

The flow in the local scour holes is characterized by a large Reynolds number and a small Froude number. Table 1 shows the most important hydraulic data of the local scour holes.

	LS1	LS2	LS3	
q (specific discharge)	0.0996	0.1188	0.1035	m^2/s
a_0	0.30	0.30	0.30	m
a_η [1]	0.34	0.43	0.58	m
x_η	3.0	3.0	3.0	m
$Re = \bar{U}_0 a_0/\nu$	99.6	119	104	$* 10^3$ (-)
$Fr = \bar{U}_0/\sqrt{(g a_0)}$	0.19	0.23	0.20	(-)
k_s (upstream)	25	25	25	$* 10^{-3}$ m
k_s (downstream)	0.5	0.5	0.5	$* 10^{-3}$ m

[1]) $\beta = 0{,}20$

table 1 Hydraulic data (Local Scour holes)

4.1.1 Longitudinal flow velocity

The slope of the local scour directly after the armour layer is approximately 1:4.5 for all three scours. Probably it is not steep enough to create a reverse flow; measurements of Breusers (Wijngaarden, 1984), as well as the calculations using the k-ϵ- and DUCT-model indicate mean positive velocities near the bottom. Generally the agreement between the DUCT-results and the k-ϵ-predictions is fair, (figures A1-A6). In the acceleration zone the calculated bottom velocities by the k-ϵ-model are somewhat larger than the ones predicted by the DUCT-model.

4.1.2 Eddy viscosity

In the deceleration zone and in the relaxation zone the agreement between both models for the eddy viscosity is rather good, however, some large differences occur in the new wall-boundary layer, (figures B1, B2 and B3). There the k-ϵ-model generates significantly larger values of the eddy viscosity compared with the values based on the measurements (and DUCT-model), (Hoffmans, 1988a). If the eddy viscosity is modelled in a almost simular way as in the k-ϵ-model, the velocities computed by the DUCT-model are nearly the same as the velocities calculated by the k-ϵ-model.

4.1.3 Bed-shear velocity

After the reattachment point the bed-shear velocities (k-ϵ-model) are somewhat larger than the calculated ones by the DUCT-model, (figures C1, C2 and C3). At the outflow boundary the k-ϵ-model generates a value, which is approximately 5 to 10% too large compared with equilibrium values calculated by traditional roughness parameters, while the DUCT-predictions are 5 to 10% below these values, (table A volume 11). The relative large k-ϵ-prediction is probably due to the large value of the Von Karman's universal constant. The k-ϵ-calculations are carried out with $\kappa = 0.435$. Normally this constant takes 0.40. This results in an eight percent increase of the bed-shear velocity, because it is proportional to κ, (equation 11). The DUCT-computations are carried out with $\kappa = 0.40$.

Because the flow is accelerating and not uniform, the bed-shear velocity should tend to a somewhat larger value than the equilibrium one, which follows from the traditional roughness predictors.

The equilibrium value is determined by the roughness predictors of Darcy Weisbach and White Colebrook. Respectively these are defined as:

$$\text{Darcy Weisbach:} \qquad f = \frac{0.24}{\log^2\left[\frac{12R}{k_s + \delta/3.5}\right]} \quad ; \; u_* = \tilde{U}\sqrt{\left(\frac{f}{8}\right)} \tag{27}$$

White Colebrook: $C = 18\log[\frac{12R}{k_s + \delta/3.5}]$; $u_* = \bar{U}\frac{\sqrt{g}}{C}$ (28)

in which:

R = hydraulic radius (= a; flow depth)

$\delta = 11.6\nu/u_*$; laminar sub-layer thickness

f = roughness-parameter

The differences between the two roughness predictors appear to be negligible.

4.1.4 Pressurecoefficient (on rigid lid)

The pressurecoefficient (c_p) is defined as:

$$c_p(x) = \frac{\bar{\zeta}(x) - \bar{\zeta}_0}{0.5\rho\bar{U}_0^2} \tag{29}$$

In the deceleration zone the pressure increases, while the pressure decreases in the acceleration region, figures C1, C2 and C3. Applying a rigid lid approach this is correct, since in reality the flow depth will increase somewhat in the deceleration zone. In the accelereation zone, where the convective term $\bar{u}\frac{\partial\bar{u}}{\partial x}$ and the pressure term $\frac{\partial\bar{p}}{\partial x}$ are dominating, this can easily be verified with the equation of Bernoulli.

Bernoulli: $\bar{\zeta} + \rho\bar{U}^2/2 = \text{constant}$ (30)

4.2 Artificial dunes and trenches

DUCT-results are compared with Laser Doppler measurements, (van Mierlo and de Ruiter, 1988 and van Rijn, 1980). Table 2 gives an overview of the most important hydraulic data of the dunes and the trenches. Because the length of the dune is relatively short compared with the flow depth, the thickness of the mixing layer is relatively small and will not become equal to the local flow depth. Moreover the degree of turbulence at the top of the crest is considerably larger than the turbulence level, which is based on the local roughness of Nikuradse. The measurements are carried out in the middle of a series of dunes in which the dune heigth is significantly larger than the particle size. At the inflow boundary the eddy viscosity is not determined from the equivalent roughness of Nikuradse, see (5), (6) and (7) but determined from the measurements, (equation 31).

$$\nu_t(z) = 4\,\frac{z}{a_0}\{1 - \frac{z}{a_0}\}\left[\frac{\overline{u^1w^1}}{\partial\bar{u}/\partial z}\right]\Bigg|_{z\,=\,a_0/2} \qquad (31)$$

in which:

$\overline{u^1w^1}$ = measured turbulent shear stress (divided by ρ)
u^1 = longitudinal flow velocity fluctuation
w^1 = vertical flow velocity fluctuation
$\partial\bar{u}/\partial z$ = flow velocity gradient

The flow velocity gradient $\frac{\partial\bar{u}}{\partial z}$ in equation (31) is estimated by:

$$\frac{\partial\bar{u}}{\partial z} \approx 0.5\left[\frac{\bar{u}_{n+1} - \bar{u}_n}{z_{n+1} - z_n} + \frac{\bar{u}_n - \bar{u}_{n-1}}{z_n - z_{n-1}}\right] \qquad (n = \text{index}) \qquad (32)$$

4.2.1 Longitudinal flow velocity

In the deceleration zone close to the bottom the calculated as well as the measured velocities are negative, (figures A7 - A14). Generally the

measured ones do have a larger value. Integrating the measured flow velocity profiles, it appears that in the deceleration region the specific discharge is smaller than the overall averaged, i.e discharge which is the average for all sections. In trench T2 the integrated velocity profile at section 2 (x = 0.40 m) gives even a value which is nearly 18% smaller than the overall one. Probably this is caused by three_dimensional effects, since the depth-width ratio of the flume was 3 to 5; the width of the flume (B) is 0.5 m. In the case of the 'dune'-measurements the standard deviation of the specific discharge is much smaller (B = 1.5 m), (table C1 and C2 volume 11).

	D1	D2	T1	T2	
q	0.1102	0.1837	0.0763	0.0417	m^2/s
a_0	0.21	0.29	0.20	0.10	m
a_η [1]	-	-	0.40	0.30	m
x_η	-	-	3.0	2.0	m
$Re = \bar{U}_0 a_0/\nu$	111	184	76.3	41.7	$* 10^3$ (-)
$Fr = \bar{U}_0/\sqrt{(g a_0)}$	0.37	0.37	0.26	0.43	(-)
k_s	2.5	2.5	6.0	6.0	$* 10^{-3}$ m
D_{50} [2]	1.6	1.6			$* 10^{-3}$ m
$\nu_{t,max,0}$	1.5	1.5			$* 10^{-3} m^2/s$

[1]) $\beta = 0.20$

[2]) D_{50} = mean particle size

table 2 Hydraulic data (Dunes and Trenches)

The separation point is not well predicted by the DUCT-model. Probably this is due to the gradients of the fluctuating velocity terms (normal stress terms), which were neglected in the equation of motion, (equation 2). The agreement of the computed and measured reattachment point is fair.

4.2.2 Eddy viscosity

The eddy viscosity in each Laser Doppler measuring point is computed using the formula (33). The shear stress is defined as:

$$\tau_{t,xz} = \rho\nu_t\left[\frac{\partial\bar{u}}{\partial z} + \frac{\partial\bar{w}}{\partial x}\right] = -\rho\overline{u'w'} \qquad (33)$$

Assuming $\frac{\partial\bar{w}}{\partial x} \ll \frac{\partial\bar{u}}{\partial z}$ equation (33) simplifies into:

$$\nu_t = -\frac{\overline{u'w'}}{\frac{\partial\bar{u}}{\partial z}} \qquad \left[\frac{\partial\bar{u}}{\partial z} \text{ is estimated by 32}\right] \qquad (34)$$

Generally the agreement between the computed eddy viscosity and the measured one is rather well, (figures B4-B7). In the recirculation zone, close to the bottom, the eddy viscosity generated by the DUCT-model is very small ($\nu_t = 5.10^{-5}$ m^2/s). In the center of the mixing layer the agreement between the calculated and the 'measured' values is fair. In the wake zone the eddy viscosity obtained from the measurements does have a nearly constant value. The figures B4-B7 also show that below the center of the mixing layer the eddy viscosity is increasing. Downstream of the reattachment point, close to the bottom, measurements show relatively small values of the eddy viscosity compared with k-ϵ-predictions but also with measured values in the main flow. Here the agreement between the measured and modelled eddy viscosity (DUCT-model) is fair.

4.2.3 Bed-shear velocity

The calculated bed-shear velocity (DUCT-model) as a function of x is qualitively correct, however in the acceleration zone the deviation from the measurements is relatively large (10 to 15%), (figures C4-C7). The shear stress is defined as:

$$\tau_{t,\tau}(\alpha_b) = -\rho\overline{u'_\tau u'_n} = \rho u_*^2 \qquad (35)$$

in which:

α_b = rotation angle (bottom slope)

u^1_τ = tangential flow velocity fluctuation

u^1_n = flow velocity fluctuation in the normal direction

The (time-averaged) tangential flow velocity and the component perpendicular upon this are written by:

$$\bar{u}_\tau = \bar{u}\cos\alpha_b + \bar{w}\sin\alpha_b \tag{36}$$

$$\bar{u}_n = -\bar{u}\sin\alpha_b + \bar{w}\cos\alpha_b \tag{37}$$

Substitution of (36) and (37) into (35) gives:

$$\tau_{t,\tau}(\alpha_b) = \rho\{\overline{(u^1)^2} - \overline{(w^1)^2}\}\sin\alpha_b\cos\alpha_b - \rho\overline{u^1w^1}(\cos^2\alpha_b - \sin^2\alpha_b) \tag{38}$$

It appears that the turbulent shear stress after rotation is related not only to the turbulent shear stress ($\rho\overline{u^1w^1}$) but also to the kinetic energy ($\rho\overline{u^1u^1}$) and ($\rho\overline{w^1w^1}$).

At the crest of the dune the measured bed-shear velocity, is approximately 10 to 15% larger than the bed-shear velocity calculated according to the traditional roughness predictors. The DUCT-model gives a value which is nearly the same as the equilibrium one. It is conceivable that the bed-shear velocity should have a somewhat larger value than the equilibrium one because of the accelerating flow; the velocity profile is not logarithmic.

The overall bed-shear velocity ($u_{*,b}$) is defined as:

$$u_{*,b} = \sqrt{[gR_b i_e]} \tag{39}$$

in which:

R_b = hydraulic radius; corrected for side wall influences

i_e = energy slope (from measurements)

At the top of the crest the measured bed-shear velocity, which follows from the local velocity field, is approximately 20% smaller than the

overall one, (table B volume 11). The difference between the two 'measured' values is mainly due to the relative large energy loss (deceleration zone).

4.2.4 Shear-stress

The computed shear-stress using DUCT-results is compared to the measured (LDA) shear-stress, figures D1 and D2. In the center of the mixing layer the computed shear-stress (divided by ρ) by the DUCT-model is predicted poorly, which is mainly due to the neglect of the normal stresses in the equation of motion. Though the velocities in the mixing layer are computed reasonably compared to the measured ones, small differences can yield a relative large difference in the flow gradient $\partial\bar{u}/\partial z$. Generally the measured velocity gradient is larger than the computed one (DUCT).

Relaxation zone

In the relaxation zone the agreement between the computed (DUCT) and measured shear-stress (LDA) is fair. It indicates that the modelled eddy viscosity using equations (23) and (24) and the computed velocities by the DUCT-model are predicted well, (figures A7-B4, A9-B5). It indicates also that the eddy viscosity in the k-ϵ-model must be too large near the bottom, since the difference between the computed longitudinal flow velocity by the k-ϵ-model and the DUCT-model is marginal, (figures A1-B1, A3-B2, A5-B3).

5. Sensitivity analysis of DUCT-parameters

5.1 Angle of mixing layer (deceleration zone)

In the center of the mixing layer the eddy viscosity increases downstream of the separation point and is proportionally to the x-direction. Actually this is not correct for large values of x (deceleration zone), since the angle of the mixing layer is diminishing gradually, figure 3.

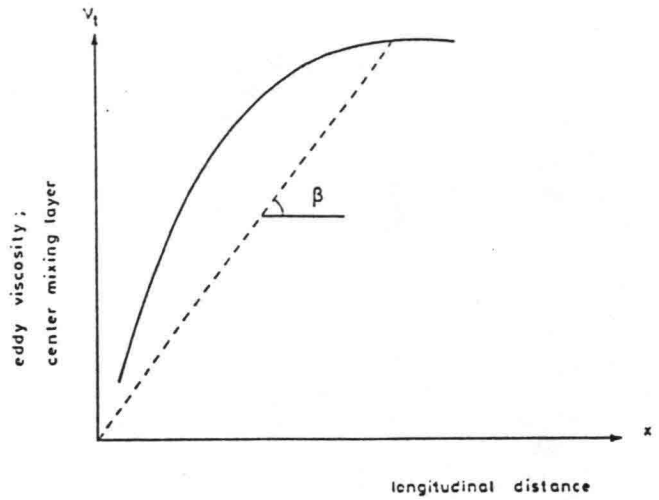

figure 3 Eddy viscosity as a function of x

Assuming β is a universal constant ($\beta = 0.20$), a correction can be carried out to the eddy viscosity by varying the growth-factor ψ. If the calculation domain in horizontal direction (dune length) is relatively small compared to the initial flow depth a better simulation of the flow velocities and the eddy viscosity values will be obtained for a larger value of ψ ($\psi > 0.15$). The constants β and ψ are determined empirically with the aid of the DUCT-model. The calibrated constants are given in table 3 for several geometries.

	LS1/LS2/LS3	D1/D2	T1/T2
β	0.20	0.20	0.20
ψ	0.15	0.20	0.15

table 3 Mixing layer-angle and growth-factor; several geometries

5.2 Mixing layer parameter (deceleration zone)

By a reduction of the mixing layer parameter α_m (or an increase of the thickness of the mixing layer) the diffusion increases in the entire vertical section, while by an enlargement the diffusion is restricted to the center of the mixing layer. Then close to the bottom the value of the eddy viscosity is very small and also the heigth of the recirculation zone is relatively large. By a diminution of α_m, the length of the recirculation zone also reduces. The mixing layer parameter α_m is determined empirically with the aid of the DUCT-model and gives reasonable results for $\alpha_m = 0.25$.

6. Conclusions

In spite of relative large Froude numbers (Fr = 0.4) the velocities in the local scour holes calculated by the DUCT-model are predicted rather good compared with k-ϵ-predictions, provided the slope directly after the armour layer is not steeper than 1:4. The model is able to describe a recirculation zone, however, the location of the separation point is not well located, because of the restrictions of the model; neglect of the fluctuating velocity components (normal stresses) in the equation of motion. On the contrary the reattachment point is computed well.
The model can not generate a grid of a backward-facing step, because then the lee-side is too steep.
In the deceleration zone the agreement with k-ϵ-predictions for the eddy viscosity is reasonably, provided the mixing layer parameter α_m is equal to 0.25, the angle of the mixing layer β is equal to 0.20 and the growth-factor ψ is equal to 0.15 - 0.20. In the acceleration zone, close to the bottom, the k-ϵ-model gives relative large values of the eddy viscosity compared with measurements. After the reattachment point, where a new wall-boundary layer will develop, the eddy viscosity obtained from the measurements is relatively small compared with k-ϵ-predictions. It is not likely that the eddy viscosity is relatively large, since an accelerating flow is characterised by a suppression of the turbulence.
Generally the bed-shear velocities (DUCT-model) are somewhat smaller than k-ϵ-predictions (κ = 0.435!) and values obtained from the measurements, however, the differences are marginal.
The overall bed-shear velocity may not be compared with measurements or k-ϵ-predictions in case the energy loss due to the deceleration is relatively large. The energy loss is reflected in equation (35), while the calculated and measured bed-shear stress are related to the local flow velocity profile.
In this research project it is important that the velocities (x and z direction), the eddy viscosity and the bed-shear velocity are predicted well in view of the calculations of the bed- and suspended load. The finally goal of this project is to simulate the development of local scour holes as a function of time. Based on the present calculated

values by the flow model DUCT, the following step in this research project is to connect the DUCT-model to the morfological model SUSTRA in order to compute the sediment transport and the erosion of the bed.

References

Booy, R. (1986), Turbulence, Lecture notes, Delft University of Technology, Dept. of Civil Eng. (Dutch).

Delft Hydraulics (1987), Documentation to the computerprogram ODYSSEE, part III^{b}: mathematical and numerical description of the code Ulysse.

Hinze, J.O. (1975), Turbulence, Second edition, Mc. Graw Hill Book Co., New York.

Hoffmans, G.J.C.M. (1988a), Flow simulation by the 2-D turbulence model ODYSSEE, No 2-88, Delft University of Technology, Dept. of Civil Eng.

Hoffmans, G.J.C.M. (1988b), Damping of turbulence parameters in relaxation zone, No 10-88, Delft University of Technology, Dept. of Civil Eng.

Hoffmans, G.J.C.M. (1988c), Influence of an exponential eddy viscosity distribution on the longitudinal flow velocity, No 14-88, Delft University of Technology, Dept. of Civil Eng.

Kay, J.M. and R.M. Nedderman (1985), Fluid mechanics and transfer processes, Cambridge University Press.

Mierlo, M.C.L.M. and J.C.C. de Ruiter (1988), Turbulence measurements above dunes, Report Q789, Vol 1 and 11, Delft Hydraulics.

Rijn, L.C. van (1980), Computation of siltation in dredged trenches; semi-empirical model for the flow in dredged trenches, Report R1267-111/M1536, Delft Hydraulics.

Rijn, L.C. van (1987), Mathematical modelling of morphological processes in the case of suspended sediment transport, PhD Thesis, Delft University of Technology, Dept. of Civil Eng.

Rodi, W., (1980), Turbulence models and their application in hydraulics, IAHR-section on fundamentals of division 2, Delft.

Termes, A.P.P. (1988), Application of mathematical models for a turbulent flow field above artificial bed forms, Report Q787, Delft Hydraulics.

Vreugdenhil, C.B. (1982), Boundary-layer flow over a sloping bottom, Program DUCT, Report S488 part 11, Delft Hydraulics.

Wijngaarden, N.J. van (1984), Fundamental research to predict the development of local scours, Report M1820, (Dutch).

Appendix A: Development of a new-wall boundary layer

The turbulent boundary layer is described by the following equations. In a steady boundary layer without external force or pressure gradient these equations simplify into (hydrostatic pressure distribution):

$$\frac{\partial \bar{u}}{\partial x} + \frac{\partial \bar{w}}{\partial z} = 0 \qquad \text{(A1)}$$

$$\frac{\partial}{\partial x}\rho\overline{u^2} + \frac{\partial}{\partial z}\rho\overline{uw} + \frac{\partial}{\partial z}\tau_{t,xz} = 0 \qquad \text{(A2)}$$

in which:

$\bar{u}$ = local-time-averaged longitudinal flow velocity

$\bar{w}$ = local-time-averaged vertical flow velocity

x = longitudinal distance

z = vertical distance

ρ = density fluid

$\tau_{t,xz}$ = turbulent shear stress

The thickness of the boundary layer (δ_w) as a function of the flow direction can be obtained by an integration of the equation of continuity and motion. Integration of the equation of continuity (A1), using the Leibniz's theorem for differentiation of an integral, yields:

$$\int_0^{\delta_w} \frac{\partial \bar{u}}{\partial x}dz + \int_0^{\delta_w} \frac{\partial \bar{w}}{\partial z}dz = \frac{d}{dx}q(x) - \bar{u}(x,\delta_w)\frac{d}{dx}\delta_w(x) + \bar{w}(x,\delta_w) \qquad \text{(A3)}$$

in which $\bar{u}(x,\delta_w)$ en $\bar{w}(x,\delta_w)$ are the flow velocity components at the heigth of the outer edge of the boundary layer, while $q(x)$ represents the specific discharge in the boundary layer.

$$q(x) = \int_0^{\delta_w} \bar{u}(z)dz \qquad \text{(A4)}$$

In an analogous way the integration of the momentum equation (A2) (divided by ρ) gives:

$$\frac{d}{dx}[\bar{u}(x,\delta_w)\{q(x) - \bar{u}(x,\delta_w)\theta(x)\}] - \bar{u}^2(x,\delta_w)\frac{d}{dx}\delta_w(x) + \bar{u}(x,\delta_w)\bar{w}(x,\delta_w) = \frac{\tau_0}{\rho}$$

in which $\theta(x)$ represents the momentum thickness of a boundary layer.

$$\theta(x) = \int_0^{\delta_w} \frac{\bar{u}}{\bar{u}(x,\delta_w)}\{1 - \frac{\bar{u}}{\bar{u}(x,\delta_w)}\}dz \qquad (A6)$$

τ_0 is the shear stress, which is exerted by the wall to the fluid.

$$\tau_0 = \tau_{t,xz}(z = 0) = \rho u_*^2 \qquad (A7)$$

Assuming that the shear stress is approximately equal to zero at the outer edge of the boundary layer, elimination of $\bar{w}(x,\delta_w)$ in (A3) and (A5) gives:

$$\bar{u}^2(x,\delta_w)\frac{d}{dx}\theta(x) = u_*^2 \qquad (A8)$$

Using the integration formula (A9)

$$\int z^n(\ln z)^m dz = \frac{z^{n+1}(\ln z)^m}{n+1} - \frac{m}{n+1}\int z^n(\ln z)^{m-1}dz \quad (n \neq -1) \qquad (A9)$$

substitution of a logarithmic flow velocity profile into (A6) yields:

$$\frac{d}{dx}[\delta_w(x)\frac{\{L(x) - 2\}}{L^2(x)}] = \frac{\kappa^2}{L^2(x)} \qquad (A10)$$

in which:

$L(x) = \ln(\delta_w/z_0)$; roughness parameter

κ = Von Karman's universal constant

The change of L to x is small compared with the change of δ_w itself, so equation (A10) reduce to:

$$\frac{d}{dx}\delta_w(x) = \frac{\kappa^2}{L_x - 2} \qquad (A11)$$

The new wall-boundary layer increases with:

$$\delta_w(x) = \frac{\kappa^2 x}{L_x - 2} \qquad \text{(A12)}$$

The value of L_x ranges from 5 to 11, so the relative growth of the boundary layer $\kappa^2/(l_x - 2)$, ranges from 1/20 to 1/50. Equation (A12) shows that the boundary layer thickness increases proportionally to the flow direction. Actually the growth of the thickness, $d\delta_w/dx$, will decrease downstream of the re-attachment point. In case of a rougher bottom the boundary layer will grow faster.

It is important to note that the above mentioned assumptions are not quite correct (close to the re-attachment), since the pressure is not constant but varies slightly in the longitudinal direction and the shear stress at the outer edge is not equal to zero. Close to the re-attachment point the pressure gradient is positive and immediately after that the pressure will fall, figure 4.

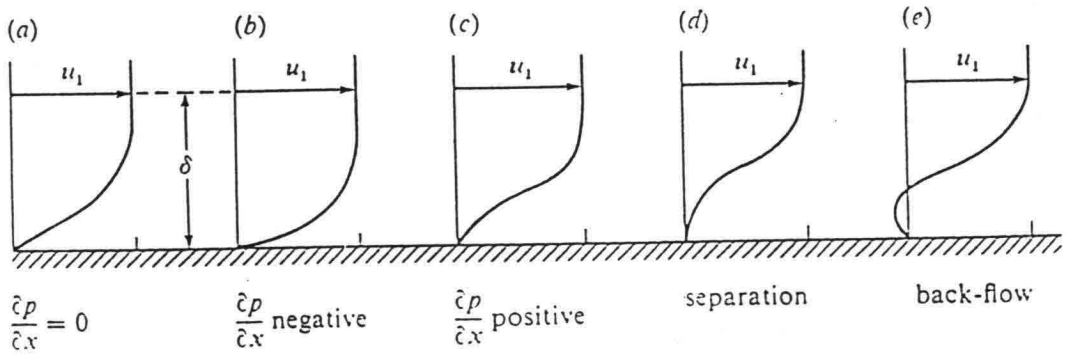

figure 4 Effect of pressure gradient on velocity profile